TECHNICAL FEATURE

AN ADAPTIVE FEEDFORWARD AMPLIFIER FOR WCDMA BASE STATIONS USING IMPERFECT SIGNAL CANCELLATION

This article describes a new adaptive feedforward amplifier for a WCDMA system using an imperfect signal cancellation. Due to the complicated signal statistics, the distortion generated by the error amplifier is significantly reduced by an imperfect signal cancellation. Therefore, the performances of feedforward amplifiers are improved with this new adaptation technique, especially for modulated signals with a high peak-to-average ratio. For verification, a 2.14 GHz feedforward amplifier, with 80 W output power, has been implemented and tested with digital control circuits. The results, compared to a perfect signal cancellation, show more than 7 dB improvement of adjacent channel leakage ratio (ACLR) at 80 W output power. The amplifier efficiency is also improved from 7.5 to 9 percent for the same ACLR.

As wireless systems evolve from second- to third- or fourth-generation, the linearity, efficiency and bandwidth requirements for power amplifiers become more stringent. Many techniques, including feedforward, envelope feedback and manifold types of predistorters, have been employed to effectively satisfy these performance requirements and to reduce the production costs for various system applications. Feedforward is generally known as the best performing linearization technique for linear power amplifiers at RF frequencies. Many previous works for various implementations and analyses of feedforward type linearizers have been reported.[1–11]

Distortion cancellation in the feedforward amplifiers is based on the subtraction of two signals. The degree of cancellation is mainly determined by the amplitude and phase balances of the signals over the bandwidth of interest.[2,3] However, due to the high peak-to-average ratio (PAR) of the error signal extracted

YOUNG YUN WOO, YOUNGOO YANG, JAEHYOK YI, JOONGJIN NAM, JEONGHYEON CHA AND BUMMAN KIM
Pohang University of Science and Technology (POSTECH)
Korea

at the first loop, the error amplifier is easily saturated and the distortion generated by the error amplifier limits the error cancellation capability of the feedforward amplifier. This problem becomes more serious as the PAR of a signal or the number of carriers is increased. Hence, a larger-size error amplifier is required to amplify the error signal without generating any significant distortion. However, the large-size error amplifier causes various problems of cost, heating and efficiency, etc.

It has already been addressed that a perfect signal cancellation in the first loop of the feedforward amplifier is not an optimum solution for minimizing the output error level.[4] In other words, the error amplifier can generate less distortion signals when an input signal with imperfect signal cancellation is applied. But Larose and Ghannouchi[4] describe numerically the phenomenon without any analysis about its cause. Also, the authors did not present a concrete adaptation plan to apply the mechanism and offer an experimental validation. An analysis for the mechanism and a method to utilize this benefit have not been explicitly studied yet. To clearly understand the operation mechanism, the effects of an imperfect signal cancellation using multi-tone and WCDMA signals have been analyzed and simulated. Also, to utilize this benefit, a new merged adaptive control method, which optimizes the signal cancellation level for the best linearity of the feedforward amplifier, has been implemented. For the experiments, a 2.14 GHz digitally controlled feedforward amplifier with 80 W output power for WCDMA base stations has been built and tested. The optimally merged control technique has been compared with the conventional method,[5,6] using down-link 16-channel WCDMA signals in both single- and multi-carrier cases.

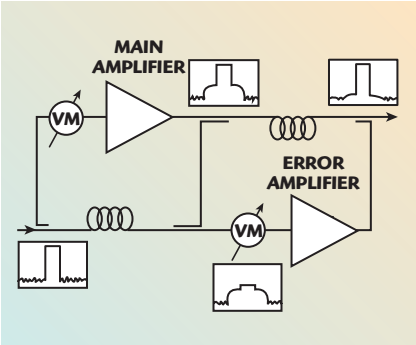

Fig. 1 Simplified block diagram of a conventional feedforward amplifier.

EFFECTS OF AN IMPERFECT SIGNAL CANCELLATION IN A FEEDFORWARD AMPLIFIER

Basic Formulation for Signal Cancellation Process

Figure 1 shows a simplified block diagram of a feedforward amplifier. The feedforward amplifier has two cancellation loops: the signal cancellation loop (or first loop) and the error cancellation loop (or second loop). In the signal cancellation loop, the subtraction of the input signal component from the coupled output signal of the main amplifier provides the pure error signal. This error signal is amplified by the error amplifier and then cancels the distortion component of the amplifier output by direct subtraction in the error cancellation loop. This subtraction nature of the feedforward method inherently requires a tight tolerance for the amplitude and phase mismatches of the two loops.

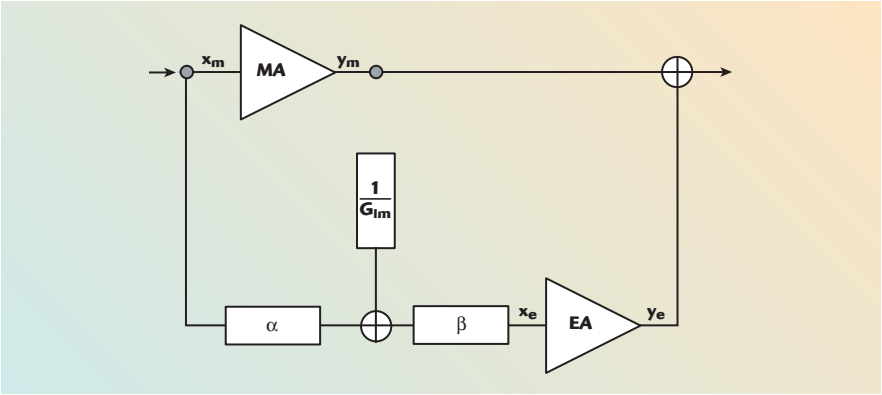

Fig. 2 Equivalent circuit diagram for the analysis of a feedforward amplifier.

Figure 2 is an equivalent system block diagram to analyze the effect of imperfect signal cancellation on the linearity. The main (MA) and error (EA) amplifiers are modeled only with third-order nonlinear coefficients for simplicity.

$$y_m = G_{1m}x_m + G_{3m}x_m^3 \qquad (1)$$

$$y_e = G_{1e}x_e + G_{3e}x_e^3 \qquad (2)$$

where

x_m = input signals of the main amplifiers

x_e = input signals of the error amplifiers

y_m = output signals of the main amplifiers

y_e = output signals of the error amplifiers

Generally, the envelope modulated input signal is expressed by

$$x_m = e(t)\cos(\omega_0 t) \qquad (3)$$

where

$e(t)$ = an envelope signal

The phase modulation is not considered because it is not important in the analysis of the nonlinear behavior. Then, the band-limited input signal of the error amplifier can be easily derived from Equations 1 and 3.

$$x_e = \beta\left\{(\alpha+1)e(t) + \frac{3}{4}\frac{G_{3m}}{G_{1m}}e(t)^3\right\}\cos(\omega_0 t) \qquad (4)$$

where

α = amplitude control coefficient to determine the signal cancellation levels

β = amplitude control coefficient to determine the error cancellation levels

The optimum value of β can be approximated to be 1, when G_{1e} is equal to G_{1m}. Then, the output signal of the error amplifier can be represented by simple forms. After gathering them to have the same exponent of envelope signal in groups, the cal-

culated output envelope signals are represented as

$$y_e\Big|_{e(t)} = G_{le}(\alpha+1)e(t) \qquad (5a)$$

$$y_e\Big|_{e(t)^3} = \frac{3}{4}\left\{G_{le}\frac{G_{3m}}{G_{1m}} + G_{3e}(\alpha+1)^3\right\}e(t)^3 \qquad (5b)$$

$$y_e\Big|_{e(t)^5} = \frac{27}{16}G_{3e}\frac{G_{3m}}{G_{1m}}(\alpha+1)^2 e^5 \qquad (5c)$$

$$y_e\Big|_{e(t)^7} = \frac{81}{64}G_{3e}\left(\frac{G_{3m}}{G_{1m}}\right)^2(\alpha+1)e(t)^7 \qquad (5d)$$

$$y_e\Big|_{e(t)^9} = \frac{81}{256}G_{3e}\left(\frac{G_{3m}}{G_{1m}}\right)^3 e(t)^9 \qquad (5e)$$

Here, Equation 5a represents the uncancelled main signal and the first term of Equation 5b describes the error signal generated by the main amplifier, and is employed to cancel the output error signal. The remaining terms are the distortions generated by the error amplifier and should be minimized.

TABLE I

AMPLIFIER MODEL PARAMETERS

Coefficient	*Value*
G_{1m}	223.6
G_{1e}	223.6
G_{3m}	–27.95
G_{3e}	–1117.97

Fig. 3 Output power level of error or distortion terms at the output of the error amplifier for the two-tone case.

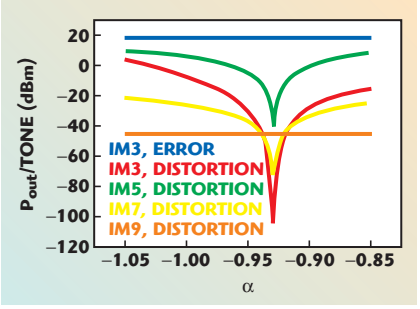

Unfortunately, the envelope signals with higher exponents have some lower order components. In other words, $e(t)^3$ contains a little fraction of e(t) component in most cases, which makes it difficult to calculate the unwanted distortion signal level generated by the error amplifier. However, the distortion terms of the third, fifth and seventh powers of e(t) are very strong functions of the signal cancellation coefficient α. Hence, it can be intuitively guessed that the distortion terms generated by the error amplifier could be cancelled out by properly adjusting α, resulting in a more linear operation of the error amplifier.

Calculation of Error Cancellation Level for Multi-tone and WCDMA Signals

To determine the effect of imperfect signal cancellation, the calculation has been performed based on the equations derived previously. For multi-tone cases, the distortion terms of the error amplifier output can be calculated with some time consuming manipulations of equations. The envelope signals of the two- and four-tones, which have the same amplitudes and identical tone-spacings of $2\omega_1$, with suppressed carrier modulation, are given as

$$e(t)\big|_{2\text{-tone}} = 2A\cos(\omega_1 t) \qquad (6)$$

$$e(t)\big|_{4\text{-tone}} = 2A\{\cos(\omega_1 t)+\cos(3\omega_1 t)\} \qquad (7)$$

where

A = amplitude of each tone

By substituting Equations 6 and 7 in equations 5a to 5e, the output power of each intermodulation (IM) term

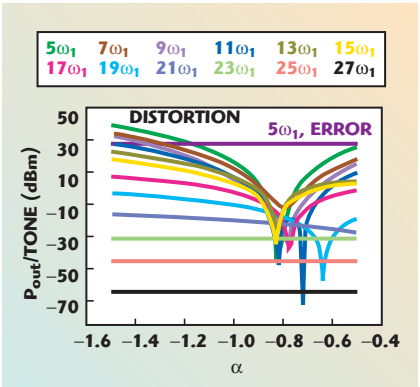

Fig. 4 Output power levels of error and distortion terms at the output of the error amplifier for the four-tone case.

can be calculated as parameters of the reference attenuation coefficient α, which determines the signal cancellation level.

For a meaningful analysis, the G coefficients are extracted from the experimental setup. The extracted parameters used in this calculation are shown in ***Table 1***. The coefficients of the main amplifier have been determined to have a third-order intercept point (IP3) of 8000 W. The coefficients of the error amplifier have been determined to have a 200 W IP3, which is 40 times smaller than for the main amplifier because the error amplifier is four times smaller than the main amplifier and a 10 dB output coupler is used in the experiments. The simulations have been carried out with an output power of 100 W for two-tone, four-tone and WCDMA cases.

Figure 3 shows the calculated output powers of each IM term for the two-tone case. IM3, IM5 and IM7 distortions vary very rapidly according to the signal cancellation level controlled by the coefficient α, while IM9 is almost constant. The optimum value of α, which makes the distortions minimum, is approximately –0.93 for this case. The calculation becomes more complicated for the four-tone signal input because the IM terms are distributed from $27\omega_1$ to ω_1. The calculated powers of each out-of-band IM term ($27\omega_1$ to $5\ \omega_1$, designated by "distortion") and the most significant error signal component ($5\omega_1$, designated by "error") for the error amplifier are plotted with their respective frequency indices in ***Figure 4***. The optimum value of α for this case becomes approximately –0.8, where the overall distortion is minimum.

In the calculated results, the optimum value of α is quite different from the α for the perfect signal cancellation. The residual main signal has a special polarity requirement to cancel out the distortion signal generated by the error amplifier. From Equation 5, the mechanism of the linearity improvement using the imperfect signal cancellation can be explained. The intermodulation (IM) terms of the error amplifier are generated by the mixing of two input signal components, that is, the residual main signal and error signal. Since

the two signals are correlated, the distortions can be minimized by optimizing α. If AM-to-PM conversion is considered, G_{3m} and G_{3e} have phase terms, and perfect cancellation is harder; however, the cancellation mechanism will work identically.

For the WCDMA signal, a calculation to acquire results similar to the multi-tone cases may be formidable. Hence, a simulation with the same amplifier models has been performed using Agilent's ADS 3GPP design library. The simulated results are presented in ***Figure 5***. The spectral powers (2.5 MHz offset from the center frequency and 30 kHz resolution bandwidth (RBW)) of the error generated by the main amplifier and the distortion signals generated by the error amplifier with α as a parameter are shown, as well as the total input power of the error amplifier to quantify the signal cancellation levels. The error cancellation capabilities of the feedforward amplifier, which are determined by the difference between the error signal and distortion of the error amplifier, become 28.5 dB for the optimum imperfect signal cancellation point, which is 15.65 dB less than that for the perfect signal cancellation point. ***Figure 6*** shows the power spectral densities (PSD) for the optimum imperfect cancellation and perfect cancellation cases, which are collected from the distortion level minimum and the total input power minimum points in the previous figure, respectively. The optimum value of α is approximately –0.825 for the WCDMA case.

Fig. 5 Spectral powers of the error and distortion signals at the output of the error amplifier.

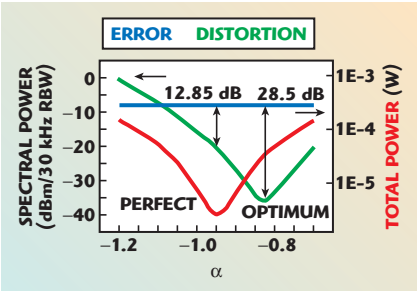

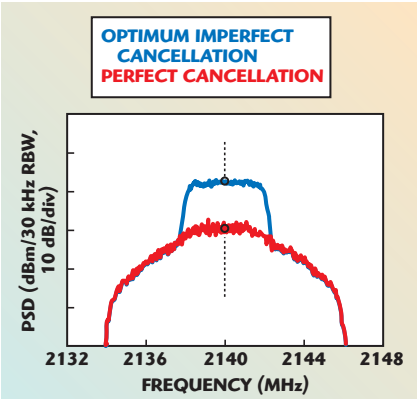

Fig. 6 Power spectral density for optimum imperfect cancellation and perfect cancellation cases.

NEW ADAPTIVE CONTROL SCHEME

To adopt the beneficial effects of the imperfect signal cancellation on suppressing the distortion generated by the error amplifier in a very simple manner, the usual four adaptive control parameters (two for the first loop and another two for the second loop controls) of the feedforward amplifier are sequentially adjusted to minimize the final output error level. ***Figure 7*** shows the simplified block diagrams to compare a new adaptation technique using imperfect signal cancellation with the conventional one. The conventional method is also used to get an initial adaptation step for the new adaptation technique. The adaptation algorithm loading this simple technique can lead to the optimum imperfect signal cancellation point described in the previous section.

Fig. 7 Simplified block diagrams of adaptive feedforward amplifiers; (a) conventional method and (b) the new adaptive method.

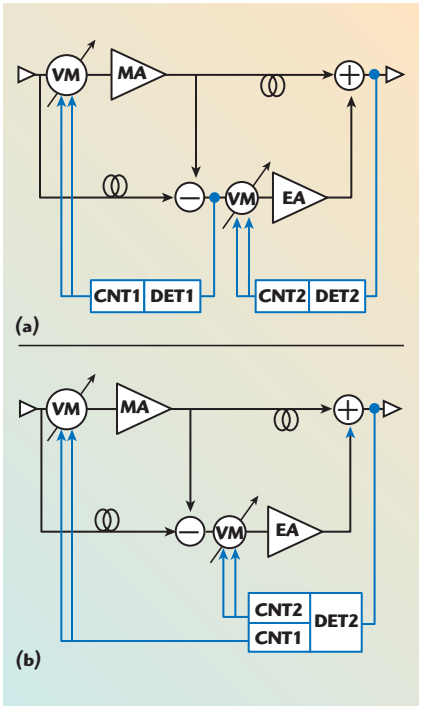

An execution flow of the proposed adaptation process is shown in ***Figure 8***. The algorithm used in this experiment is based on the modified power gradient with an adaptive delta-modulation.[5] The adaptation flow consists of two steps. Step 1 is required to search for the initial control voltages of the two vector modulators, and is identical to the conventional adaptation. After the convergence of step 1, the control is handed over to step 2. Then, all control parameters of both the first loop and second loop are sequentially adjusted to optimize the error cancellation level monitored using DET2.

IMPLEMENTATION AND EXPERIMENTAL RESULTS

Implementation

To validate the proposed adaptive control scheme, a 2.14 GHz adaptive feedforward amplifier with 80 W average output power for a down-link 16-channel WCDMA signal has been implemented. The overall main amplifier module has been designed to deliver more than a 100 W average WCDMA signal with 30 dBc ACLR at 2.5 MHz offset and 65 dB of gain. The final stage of the main amplifier has been configured to have 720 W PEP by a four-way combination of 180 W PEP amplifiers using Motorola's MRF21180 LDMOS FETs. The error amplifier module has more than 65 dB of gain and its power capacity is four times less than that of the main amplifier.

For this system, the vector modulator has been fabricated with the series

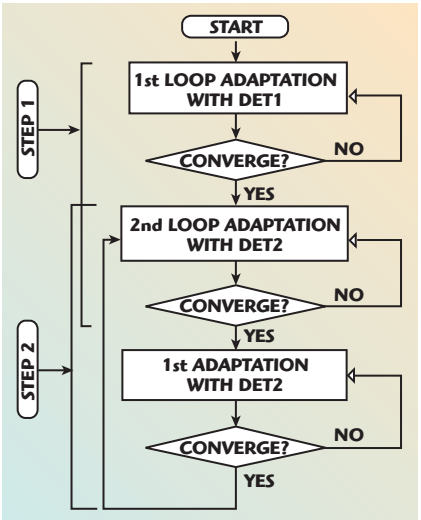

Fig. 8 Flow chart of the proposed adaptation process.

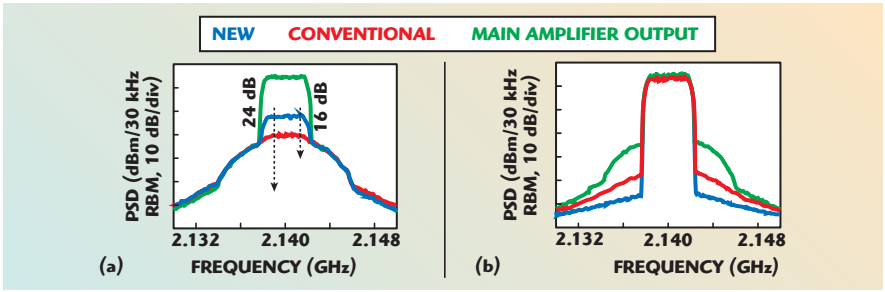

Fig. 9 PSDs with a single-carrier WCDMA signal for both the new and the conventional adaptation methods at 49 dBm output power; (a) signal cancellation level and (b) error cancellation level.

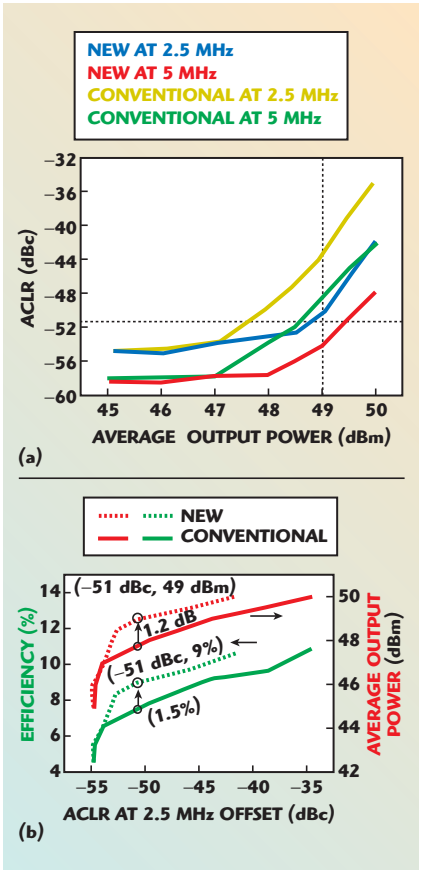

Fig. 10 Adaptive control results (a) for ACLRs at 2.5 and 5.0 MHz offsets vs. average output power and (b) for efficiency and average output power vs. ACLR at 2.5 MHz offset.

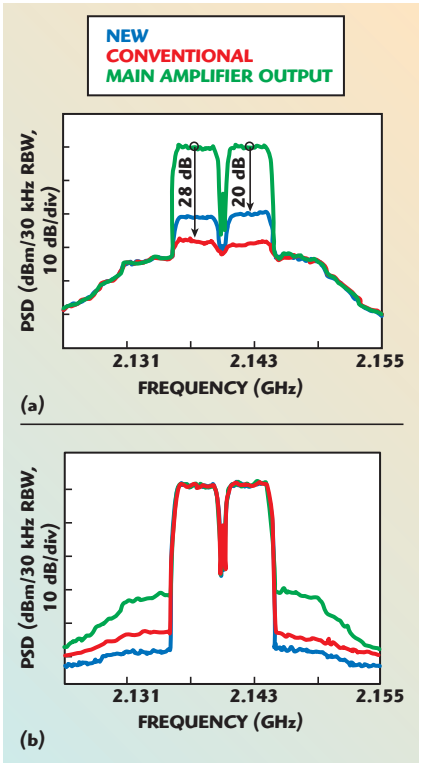

Fig. 11 PSDs with a two-carrier signal for the new and conventional adaptation methods at 47 dBm output power; (a) signal cancellation level and (b) error cancellation level.

connection of a reflection type attenuator and phase shifter using 3 dB hybrid couplers, PIN diodes and varactor diodes. The first loop delay has been compensated by a coaxial delay line and the second loop delay has been compensated by a delay filter, which has about 15 ns of delay and 0.9 dB of loss. For the conventional and new adaptation controls, a pilotless error power detection method is employed. For the detection, the RF signal is down-converted to a proper IF band to filter the main signal components out. The adaptation algorithms described in the new adaptive control scheme section were coded and installed. The adaptive control programs have been run using a low cost micro-controller based on Intel's 80C196KC CPU, two-channel ADCs and four-channel DACs. Many other digital in and out ports are also controlled to detect faults, to control the PLL frequency synthesizer for error detection, and to provide alarm and protection signals.

Experimental Results

Experiments have been performed to verify the new adaptive control scheme based on imperfect signal cancellation. Conventional and new adaptive control algorithms have been executed to optimize the linearity of a 2.14 GHz feedforward amplifier with 80 W output power using single- and multi-carrier WCDMA signals. The results for the conventional and new adaptation controls are compared. ***Figure 9*** shows the the PSDs of the signal cancellation levels and error cancellation levels of the two cases. Due to the imperfect signal cancellation, the PSD of the new adaptive control method is 8 dB higher than that of the conventional case. The error cancellation is improved by 7 dB to –51 dBc from –44 dBc of ACLR at 2.5 MHz offset at 49 dBm of average output power. ***Figure 10*** summarizes the overall adaptation experiments with a single-carrier WCDMA signal. The ACLRs at 2.5 and 5 MHz offsets for the two cases are compared for the various average output power levels. The amplifier adopting the proposed merged control method delivers approximately 49 dBm of the average output power with –51 dBc ACLR specification, which is about a 1.2 dB improvement of average output power compared with the conventional case. The power performance of the new feedforward amplifier fully satisfies the commercial specifications for WCDMA base stations. The efficiency and average output power for the various ACLRs at 2.5 MHz offset are also shown. The efficiency of the new method at ACLR = –51 dBc is about 9 percent, while that of the conventional control is 7.5 percent.

Figure 11 shows the results for the two-carrier WCDMA signal tests. The signal cancellation levels monitored at the error amplifier input are approximately 20 and 28 dB for the new and conventional cases, respectively. The ACLRs at 5 MHz offset with 47 dBm of the average output power are approximately –50.3 dBc for the new method, which is very close to the source signal level and is about a 6 dB improvement from the conventional adaptive control. The optimum imperfect cancellation point can be easily found by referring to the minimum output error level during the adaptive control, and the new adaptation algorithm always converges to the optimum point for both single- and multi-carrier WCDMA signals.

The experimental results clearly show that the new adaptive method

provides superior performance by using only the special adaptation program without any additional hardware. Thus, the new method can produce a feedforward power amplifier at a lower cost.

CONCLUSION

For signals with a high PAR, the premature saturation of the error amplifier of the feedforward system can be a major performance degrading source. Due to the interaction between the signal and the IM terms, the distortion signal generated by the error amplifier is affected by the main signal cancellation level and can be significantly reduced with a properly imperfect signal cancellation. In this article, analyses have been conducted to describe the effect of the imperfect signal cancellation on the linearity of the feedforward amplifier. To adopt the benefit of the imperfect signal cancellation to linearization, a new adaptive control method for feedforward amplifiers with merged control of the first and second loops has been proposed.

To validate the new adaptive control method, a 2.14 GHz digitally controlled feedforward amplifier with 80 W output power for WCDMA base stations has been designed and implemented. The optimal merged control technique has been compared with the conventional method using single- and multi-carrier WCDMA signals. The new method can improve the linearity to a considerable amount for the single- and multi-carrier signals, which verifies the analyses and advantages of the proposed adaptation method. This significant linearity improvement using the proposed control scheme can be easily acquired without any additional hardware. This adaptation method can be applied to any feedforward amplifier transmitting signals with a high PAR. ■

ACKNOWLEDGMENT

The authors would like to thank Charles Gentzler and Ki Young Nam at Paradigm Wireless Systems for donating the delay filter, and Doo Hun Choi at Danam Communications for many helpful suggestions. This work was supported by the Agency for Defense Development and BK21 project of the Ministry of Education in Korea.

References

1. J.K. Cavers, "Adaptation Behavior of a Feedforward Amplifier Linearizer," *IEEE Transactions on Vehicular Technology*, Vol. 44, No. 1, February 1996.
2. Y.K.G. Hau, V. Postoyalko and J.R. Richardson, "Sensitivity of Distortion Cancellation in Feedforward Amplifiers to Loops Imbalances," *IEEE MTT-S International Microwave Symposium Digest*, June 1997, pp. 1695–1698.
3. R.J. Wilkinson and P.B. Kenington, "Specification of Error Amplifiers for Use in Feedforward Transmitters," *IEE Proceedings-G*, Vol. 139, No. 4, August 1992, pp. 477–480.
4. C.L. Larose and F.M. Ghannouchi, "Pilotless Adaptation of Feedforward Amplifiers Driven by High Stress Signals," *IEEE RAWCON Digest*, August 2001, pp. 81–84.
5. Y. Yang, Y. Kim, J. Yi, J. Nam, B. Kim, W. Kang and S. Kim, "Digital Controlled Adaptive Feedforward Amplifier for IMT-2000 Band," *IEEE MTT-S International Microwave Symposium Digest*, June 2000, pp. 1487–1490.
6. G. Zhao, F.M. Ghannouchi, F. Beauregard and A.B. Kouki, "Digital Implementations of Adaptive Feedforward Amplifier Linearization Techniques," *IEEE MTT-S International Microwave Symposium Digest*, June 1996, pp. 543–546.
7. J.S. Kenney and A. Leke, "Design Considerations for Multi-carrier CDMA Base Station Power Amplifier," *Microwave Journal*, Vol. 42, No. 2, February 1999, pp. 76–86.
8. R.G. Meyer, R. Eschenbach and W.M. Edgerley, "A Wide-band Feedforward Amplifier," *IEEE Journal of Solid State Circuits*, Vol. 9, No. 6, December 1974, pp. 422–428.
9. A. Katz, "SSPA Linearization," *Microwave Journal*, Vol. 42, No. 4, April 1999, pp. 22–44.
10. S. Narahashi and T. Nojima, "Extremely Low Distortion Multi-carrier Amplifier Self-adjusting Feedforward (SAFF) Amplifier," *IEEE International Communications Conference Proceedings*, 1991, pp. 1485–1490.
11. K. Horiguchi, M. Nakayama, Y. Sakai, K. Totani, H. Senda, Y. Ikeda and O. Ishida, "A High Efficiency Feedforward Amplifier with a Series Diode Linearizer for Cellular Base Stations," *IEEE MTT-S International Microwave Symposium Digest*, May 2001, pp. 797–800.

Young Yun Woo *received his BS degree in electronic and electrical engineering from Han-Yang University in 2000, and is currently working toward his PhD degree from Pohang University of Science and Technology (POSTECH), South Korea. His current research interests include RF power amplifier design, linear power amplifier (LPA) system design and baseband correction techniques for linearizing high power amplifiers.*

Youngoo Yang *received his BS degree in electronic engineering from Han-Yang University, and his PhD degree in electrical and electronic engineering from Pohang University of Science and Technology (POSTECH), South Korea, in 1997 and 2002, respectively. In 2002, he joined Skyworks Solutions Inc.*

Jaehyok Yi *received his MS degree in electronic and electrical engineering from Pohang University of Science and Technology (POSTECH), South Korea, in 1999. Currently, he is enrolled in a PhD course in the department of electronic and electrical engineering.*

Joongjin Nam *received his BS degree in electronic engineering from Kwangwoon University, South Korea, in 1998. He received his MS degree in electronic and electric engineering from Pohang University of Science and Technology (POSTECH), South Korea, in 2000, and is currently working toward his PhD degree.*

Jeonghyeon Cha *received his BS degree in electronics and information engineering from Chon-buk National University. He is currently working toward his PhD degree from Pohang University of Science and Technology (POSTECH), South Korea. His research interests include RF power amplifier design.*

Bumman Kim *received his PhD degree in electrical engineering from Carnegie-Mellon University. He has served as a member of the technical staff at GTE Labs Inc. and as a senior member of the technical staff at the Central Research Labs, Texas Instruments. He has been a professor of electronic and electrical engineering at Pohang University of Science and Technology (POSTECH), South Korea, since 1989. His research interests include RF power amplifiers.*